

$$j = (St)(Pr)^{1/3} = 1.4(D_i/D_p)^{0.79}/Re_i\epsilon \quad (5)$$

All properties were evaluated at bulk temperature. The standard deviation for Equation (5) is $\pm 19\%$. The effects of G and D_p' on ϵ are shown for both regimes in Figure 13. (Variation in temperature with attendant variation in fluid properties accounts for some of the scatter in this figure.)

SUMMARY OF CONCLUSIONS

1. The presence of fluidized solids can increase the rate of heat transfer from retaining wall to liquid considerably, a tripling of the coefficient having been obtained.

2. The behavior of the liquid-fluidized bed can be divided into two regimes, with the maximum coefficient for a given particle size occurring approximately at the transition.

3. The first regime at lower velocities is characterized by an appreciable vertical temperature gradient, which indicates limited axial mixing; by an increase of coefficient with mass velocity; and by a lack of any appreciable effect of particle size on coefficient. Within the limits of the experiment, results in this regime are correlated by Equations (3) or (4).

4. The second regime at higher velocities is characterized by little or no vertical temperature gradient, which is an indication of considerable axial mixing; by a decrease of coefficient with mass

velocity; and by a decrease in coefficient with an increase in particle size. Within the limits of the experiment, results in this regime are correlated by Figure 11 or Equation (5).

5. In view of the low volumetric heat capacity of the solids in comparison with that of the liquid, it would appear that heat carried by the solids is not an important factor in determining the increase in heat transfer.

ACKNOWLEDGMENT

The authors wish to express their appreciation to Schenley Laboratories, Inc., of Lawrenceburg, Indiana, for the use of their facilities. The authors also thank William Licht and Chad Gottschlich for reviewing the original manuscript and Stuart Willins, Richard Lasure, and Chung-kong Hwu for assistance in preparing the figures.

NOTATION

A = heat transfer surface, sq. ft.
 c = heat capacity, B.t.u./(lb.)(°F.)
 D = diameter, ft.
 D' = diameter, μ
 G = mass velocity, lb./(hr.)(sq. ft.)
 h = coefficient of heat transfer, B.t.u./(hr.)(sq. ft.)(°F.)
 k = thermal conductivity B.t.u./(hr.)(sq. ft.)(°F./ft.)
 Nu = Nusselt number = hD/k , dimensionless

Pr = Prandtl number = $c\mu/k$, dimensionless

q = rate of heat transfer B.t.u./hr.

Re = Reynolds number = DG/μ , dimensionless

St = Stanton number = h/cG , dimensionless

Greek Letters

Δt = temperature difference, °F.

ϵ = void fraction, dimensionless

μ = viscosity, lb./(ft.)(hr.)

Subscripts

max. = maximum

p = particle

t = tube

LITERATURE CITED

1. Brown, G. G., "Unit Operations," p. 214, John Wiley and Sons, New York (1950).
2. Caldas, Isidoro, Ph.D. dissertation, Univ. Cinn. (1955), available from University Microfilms, Ann. Arbor, Mich.
3. Dow, W. M., and Max Jakob, *Chem. Eng. Progr.*, **47**, 637 (1951).
4. Gamson, B. W., *ibid.*, **47**, 19 (1951).
5. McAdams, W. H., "Heat Transmission," 3 ed., p. 303, McGraw-Hill Book Company, Inc., New York (1954).
6. Mickley, H. S., and C. A. Trilling, *Ind. Eng. Chem.*, **41**, 1135 (1949).
7. Van Heerden, C., A. P. P. Noble, and D. W. Van Krevelen, *Ind. Eng. Chem.*, **45**, 1237 (1953).
8. Wen, Chin-Yung, and Max Leva, *A.I.Ch.E. Journal*, **2**, 482 (1956).

COMMUNICATIONS TO THE EDITOR

Flow Measurement with Ball Flow Meters

H. L. SHULMAN and K. A. VAN WORMER, JR., Clarkson College of Technology, Potsdam, New York

The measurement of the rate of fluid flow is an essential part of control in almost all chemical plants. A wide variety of metering devices have been developed for this purpose ranging from relatively simple direct reading meters, such as the rotameter, to elaborate instrumentation for metering, recording, and controlling. Recently Gradishar (2) used a simple direct reading meter for gaseous hydrogen fluoride which avoided the difficulties encountered with the glass tubes used in rotameters. The reading meter consisted essentially of a section of Saran tubing in the shape of a quarter of a circle and a ball to serve as a quantitative indicator of the flow rate.

Shulman, Stieger, and Leist (3) modified this meter by employing a semi-circular tube (Figure 1). This modification makes flow-rate measurements possible in either direction without the use of auxiliary valves and piping. In addition, the symmetry of the meter makes it possible easily to check the levelness of

the installation because the ball should rest at the zero reading when there is no fluid flowing through the meter.

A ball flow meter can easily be constructed of a piece of transparent or translucent tubing and a ball which has a density greater than that of the fluid to be metered. If translucent tubing is employed, it should be mounted so that light may pass through it to facilitate locating the ball. Suitable tube materials include glass, vinyl, Tygon, Saran, and polyethylene. Balls can be metallic: steel, aluminum, and brass or nonmetallic: glass, nylon, sapphire, etc. The wide range of materials available and the ease of constructing this type of meter should make it very useful for laboratory, pilot plant, and exploratory work.

DERIVATION OF THE BALL-FLOW-METER EQUATION

For many applications ball flow meters can be calibrated experimentally with a trial-and-error procedure employed for the selection of the tube and ball. When toxic, corrosive, inflammable, or volatile

fluids are to be metered, experimental calibration is difficult or impossible. To aid in the selection of the tube and ball and in the prediction of calibration curves, an analytic and experimental study was undertaken to determine the factors influencing the design of ball flow meters.

An equation suitable for the prediction of calibration curves can be developed. When a fluid is flowing through the meter the ball comes to rest at a position indicative of the flow rate. This position is most conveniently measured by the angle which a radius of the circle extended through the center of the ball makes with the vertical (Figure 1). The ball remains in its position because there are two equal and opposite forces acting upon it. The first is the total drag of the fluid on the ball, which tends to move the ball up the tube. The second is the force due to the component of the weight of the ball which is acting parallel to the tangent at the point of contact of the ball and tube and which tends to move the ball down the tube. Goldstein (1) has

K. A. Van Wormer, Jr., is with Tufts University, Medford, Massachusetts.

collected data indicating that the total drag on a sphere τ can be related to fluid velocity u by

$$\tau = \frac{C_d \rho_f u^2}{2g_c} \quad (1)$$

where C_d is a function of only a Reynolds number, $D_b \rho_f u / \mu$, if the flow pattern of the fluid around the sphere is not influenced by the presence of a boundary.

The force opposing the drag on the ball is a component of the net weight of the ball per unit of projected area.

$$\frac{V_b(\rho_b - \rho_f) \sin \theta}{A_b} \quad (2)$$

If $W/\rho_f A_f$ is substituted for u and the forces of Equations (1) and (2) are equated, one obtains

$$W = A_f \left[\frac{2g_c v_b (\rho_b - \rho_f) (\rho_f) \sin \theta}{C_d A_b} \right]^{\frac{1}{2}} \quad (3)$$

If a new coefficient C is equal to $1/(C_d)^{1/2}$, the ball flow meter equation is obtained in its final form:

$$W = C A_f \left[\frac{2g_c v_b (\rho_b - \rho_f) (\rho_f) \sin \theta}{A_b} \right]^{\frac{1}{2}} \quad (4)$$

A correlation for the ball flow meter coefficient must be obtained from experimental data rather than determined from the data in the literature for C_d as given by Goldstein (1) because the fluid-flow patterns around the ball in a ball flow meter are influenced by the presence of the tube wall. Employing the usual dimensional-analysis methods and assuming C is a function of D_b , D_t , ρ_f , u , and μ one finds that C is a function of two dimensionless groups, a ratio of diameters (D_b/D_t) and a Reynolds number ($D_t \rho_f u / \mu$). The final correlation of the experimental data indicates that the best correlation is obtained if C is taken as a function of (D_b/D_t) and a modified Reynolds number ($\text{Deq. } G/\mu$).

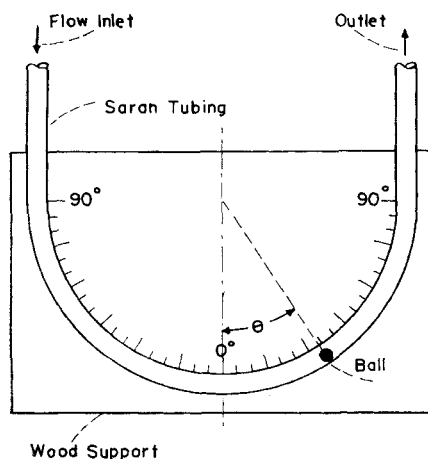


Fig. 1. Diagram of ball flow meter.

APPARATUS AND PROCEDURE

The apparatus employed for the experimental determination of the meter coefficient, shown in Figure 1, consists of a loose

ball in a piece of Saran tubing of uniform circular cross section. The tube is supported in a semicircular groove of 7-in. radius milled in a sheet of plywood and backed by glass and a light to facilitate reading of the position of the ball with the attached protractor.

The diameter of the tubing is checked for uniformity and calculated from the weight of water required to fill a measured length of tubing. Ball diameters are measured with a micrometer, the balls are weighed, and the densities are calculated.

The meter is leveled by bringing the ball to an angle of 0 deg. with no fluid flowing. Water flow from a constant-head tank or air flow from a compressed air line is maintained at a constant rate through the meter by the use of a screw clamp on a section of rubber tubing attached to the inlet side of the Saran tubing. When constant conditions are established, the temperature of the fluid, the meter reading in degrees, and the flow rate are noted and recorded. When water is used, flow rates are determined by noting the time required to collect a given weight in a galvanized container placed on a platform scale; when air is used, the volume is measured with calibrated wet and dry gas meters.

To calculate C from the experimental data, Equation (4) was modified by substituting for A_b , A_f , and v_b their respective equivalents $(\pi/4)(D_b^2)$, $(\pi/4)(D_t^2 - D_b^2)$, and $(\pi/6)(D_t^3)$, with appropriate conversion factors to obtain the working equation

$$C = \frac{W}{0.01029[(\rho_b - \rho_f)(\rho_f)(D_b')(\sin \theta)]^{\frac{1}{2}}(D_t'^2 - D_b'^2)} \quad (5)$$

Data were obtained for three tube diameters (0.1565, 0.268, and 0.419 in.) with two fluids (air and water), three ball materials (aluminum, brass, and nylon), and various ball diameters as tabulated on Figure 2.

Meter readings were kept between 9 and 60 deg. Above 60 deg. the erratic behavior of the balls makes it difficult to obtain reliable data.

CORRELATION OF DATA

Several methods of correlation were attempted, but the best results were obtained when $C(D_b/D_t)^{-0.15}$ was plotted vs. a Reynolds number ($\text{Deq. } G/\mu$). Figure 2 shows the data obtained with three different tube diameters, a variety of balls, and air and water as the metered fluids. Data for a total of 199 runs are

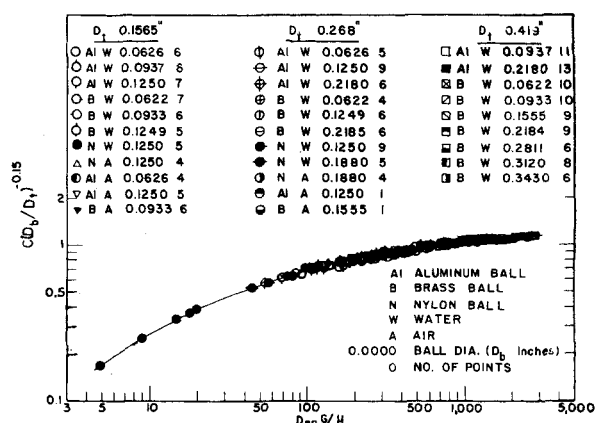


Fig. 2. Correlation of experimental data.

shown to define one smooth curve. At the higher Reynolds numbers the data fit the curve so well that it is impossible to distinguish the individual points. The excellent correlation obtained for such a wide variety of conditions indicates that Equation (4) and the correlation should be reliable for the prediction of calibration curves for ball flow meters for conditions other than those covered by the experimental work. The data presented were obtained with a 7-in.-radius meter. Additional work done with meters of radii up to 48 in. showed no effect of varying radius. In the construction of these meters it would be wise to avoid radii which are short enough to cause flattening of the tube.

DESIGN OF BALL FLOW METERS

The design of a ball flow meter involves the selection of a ball and tube and the calculation of a calibration curve. The selection of the proper materials of construction will be omitted here because it is similar to the choice of materials for any other piece of equipment handling the same fluid. To illustrate the use of the ball-flow-meter equation, a solution for a typical design will be outlined.

The specifications call for the design of a ball flow meter to meter water at 25°C. flowing at a rate of about 70 lb./hr. For this service a brass ball with a density of 528 lb./cu. ft. and a diameter 0.5 of the tube diameter will be used. Any transparent or translucent plastic tube will be suitable for this service. As an approximation C will be assumed equal to 1.0, and an angle of 25 deg. will be used as a midscale reading to allow for readings on either side of 70 lb./hr. Since $D_t' = 2D_b'$, Equation (5) can be solved for D_b' to give

$$D_b' = 0.127 \text{ in.}$$

In order to employ standard sizes a ball with a 0.125-in. diameter and a tube with a 0.250-in. internal diameter will be used. To prepare a calibration curve for this ball and tube several values of W are selected,

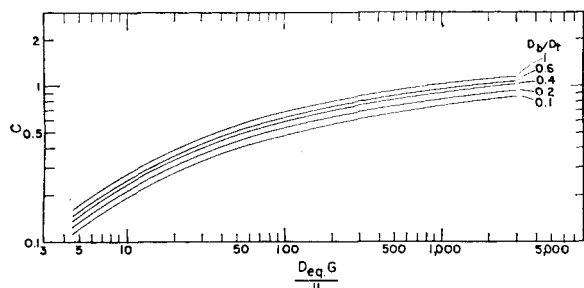
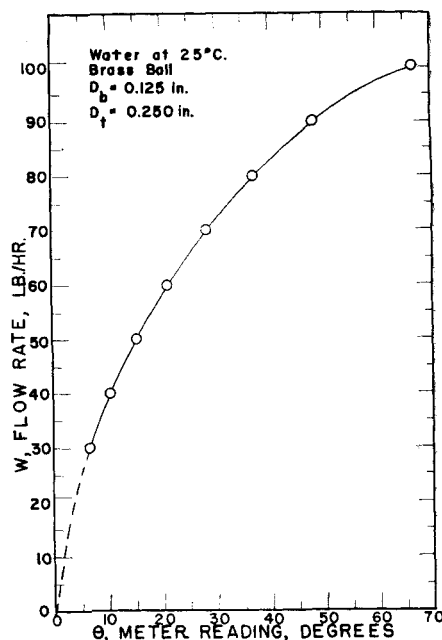


Fig. 3. Design chart for ball flow meters.

Fig. 4. Calibration curve for sample design.



and the corresponding values of $\text{Deq. } G/\mu$ are calculated. From Figure 3 the values of C , corresponding to a D_b/D_t of 0.5 and the appropriate values of $\text{Deq. } G/\mu$, are obtained. Equation (4) or (5) may now be used to obtain values of $\sin \theta$, from which θ is obtained. The calibration curve is shown on Figure 4.

NOTATION

A_b = projected cross-sectional area of ball, sq. ft.
 A_f = free area for flow of fluid between ball and tube, sq. ft.
 C = ball-flow-meter coefficient, dimensionless
 C_d = drag coefficient for spheres, dimensionless
 D_b = ball diameter, ft.
 D_b' = ball diameter, in.
 Deq. = equivalent diameter for use in

the Reynolds number, $(D_t - D_b)$, ft.
 D_t = tube diameter, ft.
 D_t' = tube diameter, in.
 G = mass flow rate based on free area (A_f), lb./sec. (sq. ft.)
 g_c = conversion factor, (lb.-mass)(ft.) / (lb. force)(sec.) (sec.)
 T = temperature of fluid, °C.
 u = fluid velocity, ft./sec.
 v_b = volume of ball, cu. ft.
 W = fluid flow rate, lb./sec.

Greek Letters

θ = meter reading, angle from vertical, deg.
 μ = fluid viscosity, lb./ft. (sec.)
 ρ_b = ball density, lb./cu. ft.
 ρ_f = fluid density, lb./cu. ft.
 τ = drag on sphere per unit of projected area, lb.-force/sq. ft.

LITERATURE CITED

1. Goldstein, S., ed., "Modern Developments in Fluid Dynamics," Oxford Univ. Press, London (1938).
2. Gradishar, F. J., *Chem. Eng.*, **57**, No. 10, 122 (1950).
3. Shulman, H. L., F. M. Stieger, and A. R. Leist, *ibid.*, **60**, No. 2, 173 (1953).

Absorption into an Accelerating Film

L. E. SCRIVEN and R. L. PIGFORD

University of Delaware, Newark, Delaware

If the velocity field in the neighborhood of the gas-liquid interface is not uniform in a steady state apparatus such as a wetted-wall column or a jet, then the rate of absorption is no longer given by the simplest form of the so-called "penetration" theory, in which the local absorption rate is assumed to be the stagnant-liquid absorption rate. Rather, a more general form of the diffusion equation must be employed in which it may not be especially convenient to replace contact distance by contact time. Since this matter does not seem to have been fully allowed for by the author of a recent communication (3), a brief discussion is given here. For the purpose of illustration, the magnitude of the acceleration end effect in a short wetted-wall column is estimated from the equations presented herein. Such an end effect was suggested by Vivian and Peaceman (4) as a possible explanation of the discrepancy between experimental and theoretical absorption rates in their columns.

The equation governing ordinary diffusion in a binary system, for constant diffusivity and mass density, is

$$\frac{\partial c}{\partial t} + (\mathbf{u} \cdot \nabla)c = D \nabla^2 c \quad (1)$$

For a short wetted-wall column or jet it is generally permissible to regard the absorbing liquid as two dimensional with infinite depth and to neglect diffusion in the direction of flow; at steady state Equation (1) then reduces to

$$u \frac{\partial c}{\partial x} + v \frac{\partial c}{\partial y} = D \frac{\partial^2 c}{\partial y^2} \quad (2)$$

where c is concentration in mass per unit volume, x and u are distance and the velocity component parallel to the interface respectively, y and v are distance and the velocity component normal to the interface respectively, and D is the diffusivity. The appropriate boundary conditions are

$$\begin{aligned} c &= c_0 \quad \text{for } x < 0, \quad y \geq 0 \\ c &= c_0 \quad \text{for } x > 0, \quad y = \infty \\ c &= c_s \quad \text{for } x \geq 0, \quad y = 0 \end{aligned}$$

where interfacial equilibrium and absence

both of heat effects at the interface and of gas-phase diffusional resistance have been assumed. At the interface $(\partial u / \partial y)_{y=0}$ will be very nearly zero (the adjoining gas exerts negligible drag upon the liquid surface), and so u may be replaced by the surface velocity u_s , provided that the penetration depth of solute gas molecules is sufficiently small. From the equation of continuity

$$v = - \int_0^y \frac{\partial u}{\partial x} dy \quad (3)$$

Hence in the region of interest, close to the interface, the normal component of velocity is approximated by

$$v = -y \frac{du_s}{dx} \quad (4)$$

and the diffusion equation becomes

$$u_s \frac{\partial c}{\partial x} - y \frac{du_s}{dx} \frac{\partial c}{\partial y} = D \frac{\partial^2 c}{\partial y^2} \quad (5)$$

If the liquid is being accelerated in the x direction, liquid elements are stretched in the x direction and suffer a corresponding shrinkage in the y direction; this causes a bulk flow of liquid toward the surface, which in the case of absorption opposes the mass flux due to the concentration gradient, but at the same time results in a steepening of the concentra-